Dermal Papilla Cells and Melanocytes Response to Physiological Oxygen Levels Depends on Their Interactions

Carla Abreu
3B's Research Group – Biomaterials, Biodegradables and Biomimetics, University of Minho, Avepark 4805-017 Barco, Guimarães, Portugal

Rui L Reis
3B's Research Group – Biomaterials, Biodegradables and Biomimetics, University of Minho, Avepark 4805-017 Barco, Guimarães, Portugal

Alexandra P Marques (apmarques@i3bs.uminho.pt)
3B's Research Group – Biomaterials, Biodegradables and Biomimetics, University of Minho, Avepark 4805-017 Barco, Guimarães, Portugal ICVS/3B's – PT Government Associate Laboratory, Braga/Guimarães, Portugal https://orcid.org/0000-0002-3222-0310

Research

Keywords: Physoxia; hair follicle; dermal papilla cells; melanocytes; cellular interactions

Posted Date: August 11th, 2020

DOI: https://doi.org/10.21203/rs.3.rs-53575/v1

Version of Record: A version of this preprint was published at Cell Proliferation on June 8th, 2021. See the published version at https://doi.org/10.1111/cpr.13013.

Abstract

Background: The specialized dermal papilla (DP) cells and the tyrosinase-active melanocytes are central players in hair growth and pigmentation, respectively. In the hair follicle (HF), oxygen levels average about 5%O_2 (physoxia) and are intimately coupled with the production of reactive oxygen species (ROS), which contribute to hair growth. Considering that oxygen and ROS might have a major role in the maintenance of the HF cellular functions, we studied the effect of physoxia over human DP cells and melanocytes (hMel) and investigated if these cells interaction altered this response.

Results: Physoxia decreased DP cells senescence and improved their secretome and phenotype, representing a reliable in vitro culture environment. Further, hMel proliferation, migration and tyrosinase activity were also enhanced, demonstrating physoxia capacity to sustain biologically relevant features. Physoxia affected DP cells alkaline phosphatase (ALP) activity, but their signalling did not influence hMel proliferation or tyrosinase activity when indirectly co-cultured. Additionally, ROS production in co-cultured cells was higher than in the respective monocultures, but lower in response to physoxia than in normoxia (21%O_2). Considering the results, we further assessed a potential link between DP cells ALP activity and ROS levels, but DP cells treatment with H_2O_2 showed that these are not directly correlated. Moreover, and given their proximity within the HF, hMel were directly cultured with DP spheroids, rendering 3D-aggregates that recreated these cells native microarchitecture and phenotype. Further, both hMel tyrosinase activity and DP cells ALP activity, their main functional indicators, as well as ROS production were higher in the 3D-aggregates cultured under physoxia than in normoxia.

Conclusions: Overall, we provide evidence that the response to physoxia differs according to hMel-DP cells interactions, and that the microenvironment recreated when they are in direct contact favours their follicular functions, including hair growth and pigmentation promoting capacity.

Introduction

Hair growth is mainly controlled by the dermal papilla (DP), the hair follicle (HF) inductive mesenchymal structure, whereas its pigmentation relies on the melanogenic activity of follicular melanocytes [1,2]. These melanocytes represent the progeny of melanoblasts residing in the bulge, which proliferate and migrate to the hair bulb, surrounding the DP and starting to produce and transfer melanin to the keratinocytes of the growing shaft [3–7]. Although the DP is considered the HF control centre, and its anatomical proximity with bulbar melanocytes implies a role also in hair pigmentation, little is known about DP cells capacity to regulate melanocytes. Rodent studies indicate that DP cells can influence melanocytes proliferation/differentiation, migration and affect pigment formation and hair coat colour [8]. In vitro studies confirmed a chemotactic effect of DP cells conditioned medium towards human melanocytes (hMel) [5], further suggesting mediation of melanocytes location and migration in the HF by DP cells. Interestingly, DP cells extracellular matrix (ECM) was also suggested to stimulate tyrosinase activity [9,10], the rate-limiting step for melanin production [11].

Oxygen (O_2) is a basic component of the tissue's microenvironment and their fluctuation can deeply affect cellular metabolism, signalling, proliferation, differentiation and reactive oxygen species (ROS) formation [12,13]. Physiological ROS play a regulatory role in several cellular signalling events [14–16] however, ROS imbalance has been linked to the etiopathogenesis of several conditions, including androgenetic alopecia and hair greying [17,18]. It is well known that ROS accumulate at supraphysiological oxygen levels [19]. Previous studies demonstrated that in cultures performed under 21%O_2 (normoxia) both HF mesenchymal (DP and dermal sheath cells) [20] and epithelial [21] populations proliferate at lower rates than when respectively cultured at 6%O_2 or 4%O_2. Moreover, under hypoxic conditions (2%O_2), DP cells viability, phenotype and inductivity are improved [18,22]. Further, hMel proliferation and melanin production are also higher at 1–5%O_2 than above normoxia [23]. Overall, these studies indicate that low oxygen levels are beneficial for DP cells and melanocytes, which seem to agree with the oxygen tension measured in the human DP (4.0-5.2% O_2) [24] or skin (average 5.3%O_2) [25]. Nevertheless, the anagen hair bulb is a ROS-enriched microenvironment [26], in which ROS directly activates proliferation and differentiation programs, stimulating hair growth [27]. Therefore, the involvement of multiple oxygen-associated responses, potentially by the different cells implicated in hair growth is expected, but yet to be elucidated.

Considering this, we investigated hMel and DP cells response to physiological oxygen levels (5%O_2, physoxia) and if this response was influenced by their interaction, aiming at mirroring their potential communication within the HF. We demonstrate that under physiological culture conditions, together with an expected decrease in ROS levels, both DP cells and hMel showed increased proliferative capacity and functionality. Interestingly, DP cells and hMel response to physoxia varied not only if these were co-cultured, but also whether they were indirectly or directly interacting. When hMel and DP cells were directly contacting in 3D cell aggregates resembling their native organization, the microenvironment recreated under physoxia favoured their highly specialized follicular functions.

Results

Physoxia reduces the negative impact of in vitro culture conditions on DP cells

DP cell cultures are typically established under normoxia, rapidly losing their native phenotype and intrinsic properties [28,29], including their key self-aggregation capacity [30,31]. Moreover, they also have a short lifespan [32] in culture, which is accompanied by morphological changes such as shifting from a small polygonal morphology to a spindle-like shape [33,34], before acquiring an enlarged morphology [18]. Therefore, we investigated if those changes also occurred under physoxia to understand how the O_2 level impacts DP cells phenotype in culture. DP cells under physoxia depicted a polygonal and less spindle-like shape and higher nuclei-to-cytoplasm ratio, as demonstrated by the significant decrease in the cells' area, perimeter and major axis length in comparison to normoxia (Fig. 1a-d). Physoxia also significantly decreased the percentage of senescent DP cells in culture (Fig. 1e) and improved their

aggregative capacity (Fig. 1f). Moreover, it enhanced cell proliferation, albeit the DNA amount at day 3 was similar in normoxia and physoxia (Fig. 1g). Interestingly, an opposite effect was observed regarding collagenous (COL, Fig. 1h) and non-collagenous (NCOL, Fig. 1i) proteins secretion under physoxia, beneficial only after 3 days in culture. Altogether, these results suggest that physoxia promotes a healthier state in cultured DP cells, which featured characteristics typically associated with low passage cells.

Physoxia enhances hMel migration, tyrosinase activity and proliferation within short culture times

Although hMel are normally cultured under normoxia, there are indications that their proliferation and tyrosinase activity are favoured under lower oxygen tensions [23]. We found that physoxia significantly increased both hMel migration (Fig. 2a) and tyrosinase activity (Fig. 2b), although this last effect was not sustained along with the culture. Similarly, significantly higher DNA levels were observed for hMel cultured under physoxia at day 3 of culture (Fig. 2c), suggesting an improved proliferative capacity. This effect was lost with the culture time, despite the high number of Ki67-positive cells (Fig. 2d). Physoxia did not seem to affect hMel morphology (Fig. 2e). Collectively, these results indicate that physoxia supports hMel functional features better than normoxia but only for short culture periods.

DP cell and hMel response to physoxia depends on their type of interaction

Although residing in close vicinity in the hair bulb and having their functions coupled to anagen [35,36], little is known about how human DP cells and hMel interact and potentially affect each other's functionality. Knowing that physoxia individually improved hMel and DP functional features after 3 days in culture, we then explored its effect when these cells were indirectly co-cultured (Fig. 3a). The co-culture with DP cells did not add to the increased hMel proliferation induced by physoxia (Fig. 3b), in opposition to normoxia. Like for proliferation, co-culture with DP cells under physoxia did not affect hMel tyrosinase activity, contrarily to normoxia, which promoted a recovery from the negative effect of the co-culture medium (Fig. 3c).

Regarding DP cells, they proliferated significantly more under physoxia than in normoxia but only when cultured in their conventional medium. Thus, the higher DNA amount detected in co-culture might be due to the medium used. This is also sustained by the results similar to the control condition, both under physoxia and normoxia (Fig. 3d). The amount of active alkaline phosphatase (ALP) cells in the co-culture was not affected by physoxia but, as for proliferation, the medium used led to a significant increase of this inductive marker. In the presence of hMel, a significant decrease of DP cells active ALP was observed under physoxia, but not in normoxia (Fig. 3e).

In the HF, hMel and DP cells are separated only by a thin and permeable basal lamina [2]. Therefore, we sought to investigate if physoxia effects were different than those observed in the indirect co-cultures, assuming a direct interaction between hMel and DP cells. When hMel were cultured with DP spheroids, they organized themselves around the spheroid in a biomimetic fashion, displaying a polarized positioning over one-half of the DP spheroid, independently of the oxygen level (Fig .3f). Highly-stable

aggregates with similar DNA content were obtained (Fig. 3g). Interestingly, both cell types phenotype was improved under physoxia, as demonstrated by a significant increase on hMel tyrosinase activity (Fig. 3h) and by the higher amount of active ALP in DP cells (Fig. 3i), respectively their main functional markers. Moreover, COL and NCOL proteins production by aggregates cultured in physoxia was significantly higher than in normoxia (Fig. 3j). Physoxia benefits hMel and DP cells functionality when both cells types are directly contacting. Interestingly, hMel response to physoxia does not seem to be indirectly affected by DP cells, while hMel signalling appears to have an impact on DP cells ALP activity.

ROS generation due to hMel and DP cells interaction does not directly correlate with DP cells functionality

During hair growth and pigmentation the bulb is a ROS-enriched environment [26], therefore in addition to the functionality of hMel and DP cells, we addressed the involvement of ROS in their response. The production of ROS by hMel was significantly lower under physoxia, although this effect was significant only for the co-cultures (Fig. 4a). Moreover, hMel in co-culture produced significantly more ROS than in the control conditions, regardless of the oxygen level. Physoxia also led to a reduction of the ROS levels in DP cells in comparison to normoxia, independently of the culture conditions (Fig. 4b). The indirect co-culture with hMel under physoxia also resulted in significantly higher amounts of ROS than in control conditions (Fig. 4b). Surprisingly, when cells were directly cultured, ROS production in physoxia was significantly higher than in normoxia (Fig. 4c), the opposite of what was observed in indirect co-cultures.

Considering that in indirect (Fig. 3e, 4b) or direct (Fig. 3i, 4c) co-cultures the effect of physoxia over the amount of active ALP and ROS followed a common trend, we then investigated if there was a correlation between these responses. For that, DP cells were treated with hydrogen peroxide (H_2O_2) to increased oxidative stress, with the ROS inhibitor *N*-acetyl cysteine (NAC) or both. Treatment with the exogenous ROS (H_2O_2) led to a significant decrease in the amount of DNA (Fig. 4d) but surprisingly, it did not affect DP cells ROS intracellular levels (Fig. 4e) while a significant decrease of active ALP was observed (Fig. 4f). Moreover, NAC pre-treatment before H_2O_2 addition further enhanced ROS production in comparison to H_2O_2 alone, but it also reduced the H_2O_2 effect on the amount of active ALP. Although it is not clear the mechanism by which H_2O_2 decreases ALP activity in DP cells, these results suggest that it is not directly correlated with an increase in ROS levels.

Physoxia and 3D co-culture supports DP cells and hMel native phenotype

To further explore both physoxia and hMel influence on DP cells hair regenerative potential, we looked at the production of a known promoter [37,38] or inhibitor factor [39] of hair induction, respectively VEGF and BMP2. In physoxia, the amount of VEGF released by DP cells was significantly higher than in normoxia independently of the culture condition (Fig. 5a). The co-culture medium negatively impacted VEGF release by DP cells, which was not overcome with the co-culture with hMel. In opposition, the amount of BMP2 in physoxia was significantly lower than in normoxia, for both co-cultures and conventional DP culture medium (Fig. 5b). As this effect was not seen in the control established with the co-culture medium, it suggests that hMel presence was essential for the observed result.

Considering hMel-DP cell aggregates 3D-architectural resemblance with the HF bulb and the observed advantages regarding their functionality under physoxia, we then investigated the rescue of cell's native-like phenotype under these conditions. The expression profile of different DP and hMel markers in the 3D-aggregates (Fig. 5c) showed that the cells display a phenotype and organization identical to the native HF (Fig. 5c, upper panel). The identification of the hMel markers tyrosinase, PMEL and MelanA, and vimentin and S100 also expressed by DP cells, showed clear compartmentalization between the cell types. Moreover, Ki67 immunolabelling confirmed a low number of proliferative cells within both cellular compartments (Fig. 5c). Noteworthy, tyrosinase expression in the cellular aggregates was higher than in conventionally cultured hMel (Fig. S1). Moreover, the in vivo predominant V2-isoform of versican [40], a DP inductive marker typically absent in 2D-cultured cells (Fig. S1) was weakly expressed in the cellular aggregates, confirming what was previously described for DP spheroids [28].

Overall, these results indicate that under physoxia DP cells inductive secretome is promoted which, in conjunction with 3D-culture conditions, allows the recovery of critical melanocytes and DP cells native markers.

Discussion

Besides ensuring overall cellular survival, oxygen levels are responsible for regulating a wide range of tissue functions, the reason why each organ, or even tissue, has its oxygenation status [12]. In the HF and skin, oxygen ranges about 5%O_2, however, the anagen hair bulb is a ROS-enriched microenvironment [26], which seems to indicate the involvement of multiple oxygen-associated responses, potentially by the different cells implicated in hair growth. Therefore, we aimed to explore DP cells and hMel response to physiological oxygen levels, and if this response was influenced by either their indirect signalling or their direct contact, as it happens in the native tissue.

When cultured at standard atmospheric levels, DP cells have a characteristic short lifespan before entering growth arrest [32] and gradually lose their native properties [1]. This has been associated with premature senescence in vitro, triggered by excessive ROS production and oxidative stress [18]. We show that DP cells cultured under physoxia featured an early-culture morphology and phenotype, characterized by decreased senescence and increased proliferative and aggregative capacity. Moreover, under physoxia ROS levels were lower, which is expected given the reduced oxygen availability for the mitochondrial respiratory chain [41], the main toxic ROS producer [42]. When exposed to excessive ROS DP cells capacity to support hair growth is severely compromised and they lose their hair inductive ability [43]. Interestingly, DP cells cultured under physoxia released higher amounts of VEGF and reduced levels of BMP2, which corresponds to the necessary trend to promote anagen induction and hair growth initiation [38,39,44,45], suggesting that physoxia stimulates DP cells inductive secretome. Further, also in agreement with what referred above to DP cells, hMel cultures under physoxia showed lower ROS levels. This was also associated with an increase of hMel migration, proliferative capacity and tyrosinase activity, confirming the results of a previous study showing higher hMel growth and pigmentation in cultures established under 1–5%O_2 [23].

During the hair growth phase, hMel mature into tyrosinase-active cells after migrating to the hair bulb and surrounding the DP, and indirect evidence suggest that DP may be involved in this process [11]. In a previous study, DP-conditioned medium was shown to enhance hMel tyrosinase activity under normoxic conditions [10]. We show that hMel tyrosinase activity in the presence of DP cells and under physoxia was higher than in normoxia, yet similar to the homotypic controls, suggesting that the influence of DP released factors on hMel do not surpass physoxia benefits. Interestingly, in our work hMel tyrosinase activity in the 3D-aggregates cultured under physoxia also correlated with a higher ECM deposition, which is in agreement with a previous study [10] that showed improved tyrosinase activity in both hMel direct co-cultured with DP cells and with their ECM. These seem to support a link between hMel tyrosinase activity and DP cells ECM, in addition to their secretome.

In the HF, DP cells are mitotically quiescent [46,47] and the differentiated tyrosinase-active hMel are less committed to cell division [6,48]. In the indirect co-cultures, hMel proliferated more in response to physoxia while DP cells remained unaffected, contrarily to the compromised proliferative capacity shown before for both DP cells and hMel cultured under normoxia [20,23]. Further, the cells proliferative capacity in the 3D-aggregates was lower than in the indirect co-cultures that were established in 2D standard conditions, evidencing a mitotic profile that more closely emulates the native behaviour.

Despite the generically accepted deleterious effects of supraphysiological ROS accumulation, there is a thin line separating beneficial and detrimental effects, which is associated to the tissues' physiological ROS levels. In the hair bulb, a transient and physiological elevation of ROS [26] is necessary to promote hair growth and differentiation programmes [27] during anagen. Interestingly, although ROS levels in co-cultured hMel and DP were lower under physoxia than in normoxia, potentially as a consequence of the lower oxygen availability, they were higher than in the corresponding homotypic controls, which was observed independently of the oxygen level. This seems to suggest that there is an indirect interaction between the two cell types that influence ROS formation. Intriguingly, and unlike what was observed in the co-cultures, in the 3D-cellular aggregates ROS generation was higher in physoxia than in normoxia. While this seems to contradict the expected relation between the available oxygen and the ROS formation, it is also known that spheroids represent a hypoxic environment [49,50]. Thus, the oxygen levels in the highly compact DP-hMel aggregates are also likely to be below 5%O_2 and lead to the formation of ROS by an alternative mechanism [19], as it was previously demonstrated to play a key role in the stimulation of DP cells inductivity [22]. Moreover, ROS increase in the 3D-cellular aggregates may also be a consequence of the improved tyrosinase activity which is, by itself, a ROS-generating oxidative step [51,52]. Moreover, albeit a direct correlation was not observed in flat cultures, in the 3D-cell aggregates both ROS levels and ALP activity were higher in physoxia than in normoxia, demonstrating that in a more complex environment the native interactions between hMel and DP cells can be better represented.

In summary, our results demonstrate that the recreation of the HF oxygen levels and the associated decrease of intracellular ROS benefit both hMel and DP cells, improving their proliferative capacity and functional features. Furthermore, we show that the type of interaction occurring between these cells also

affects their response to physoxia and that, within the 3D-aggregates, both hMel and DP cell-type functions and ROS generation are increased. Taken together, our results demonstrate that hMel-DP cells direct interaction under physiological oxygen levels has a superior capacity to recreate a microenvironment that more closely simulates the anagen bulb milieu, consequently enhancing their follicular cell-specific functions.

Materials And Methods

Cell culture

Human scalp samples were obtained from consenting patients who underwent hair transplantation procedures at Sanare Unicapilar (Porto, Portugal) and used to isolate DPs [53]. DP cells were sub-cultured on bovine collagen-coated (Sigma-Aldrich) surfaces in DMEM (Sigma-Aldrich) with 10%FBS and 1%antibiotic-antimycotic solution (Gibco). hMel were purchased from Cell Applications (San Diego, USA) and cultured in the recommended complete HEM medium. Unless otherwise stated, the cell densities used to establish the monocultures were $2x10^4$cells/cm^2 (DP cells and hMel).

Physoxia cultures were established with 5%O_2 in a hypoxic chamber (Coy O2 Control Glove Box; Coy Laboratory Products, USA). Cells cultured under normoxia were used as controls. Cells were used up to passage 4 (hMel) or passage 7 (DP cells).

To assess the link between ROS and ALP, DP cells were cultured overnight and then treated with H_20_2 (300µM, PanReac AppliChem), with NAC (1mM, Sigma-Aldrich) or with NAC for 2h before H_2O_2.

Morphology and aggregation analysis

After 3 days of culture, DP cells were fixed with 10%-formalin for 15min at room temperature (RT) and their F-actin filaments stained with Phalloidin-TRITC (0.1 mg/mL, Sigma-Aldrich) for 1h at RT. Nuclei were counterstained with 4,6-diamidino-2-phenylindole (DAPI) (1:1000, Biotium) for 15min at RT. Images (six per triplicate) were acquired with an Axio Observer microscope (Zeiss) and used for the quantification of cell area, perimeter and major axis length, with the software module "*MeasureObjectSizeShape*" of CellProfiler™ 3.0.0 [54].

Cell aggregation was analysed after 7 days of culture, after labelling the cells' nuclei with DAPI. Images (ten per triplicate) were acquired (Axio Observer, Zeiss) and analysed with the CellProfiler 3.0.0™ module "*RelabeledNuclei*". Cells were considered adjacent if the distance between their nuclei was below 8 pixels. Groups of 30 or more adjacent cells were counted as one aggregate.

Senescence-associated-β-Galactosidase assay

DP cells were seeded at a density of $1x10^4$cells/cm^2 and cultured overnight. Next day, the cells medium was replaced by serum-free DMEM and DP cells were kept in culture for 5 days. The detection of

senescence cells was performed using the Senescence β-Galactosidase Staining Kit (Cell Signaling Technology) following manufacturer instructions. Images (12 per each triplicate) used to quantify the percentage of senescent cells were taken using an AxioVert.A1 microscope (Zeiss)

Quantification of collagenous and non-collagenous proteins

The total amount of COL and NCOL proteins were quantified using the Sirius Red/Fast Green Staining Kit (Chondrex) according to the supplier instructions. DNA values were used to normalize data.

Migration assay

hMel ($4x10^4$ cells/cm^2) were seeded in 8.0µm pore size inserts (Corning) in non-supplemented HEM medium, whilst complete medium was added to the bottom well. After 48h of culture under normoxia or physoxia, cells that migrated from the insert to the bottom well were fixed with 10%-formalin (15min, RT). Images were acquired with an AxioVert.A1 (Zeiss) for quantification (12 per triplicate) or with an Axio Observer (Zeiss) microscope after staining the cells' nuclei with DAPI.

Tyrosinase activity quantification

hMel were incubated for 5min (ice) with 20mM Tris(hydroxyethyl) aminomethane (pH 7.5) containing 0.1%Triton X-100 and a protease inhibitor cocktail (1:100, Sigma-Aldrich). Cell lysates were then centrifuged at 14500rcf (10min, 4ºC) and 70µL of the supernatant transferred into transparent 96-well plates. As a substrate for tyrosinase, a 0.1% (wt/v) L-Dopa (Sigma-Aldrich) solution was prepared in sodium phosphate buffer (pH 6.8) and 140µL were added to each well. Plates were incubated for 2h at 37ºC, and the absorbance measured at 475nm using a microplate reader (Synergy HT, BioTek). Data are presented as relative tyrosinase activity after normalization with DNA values.

Co-cultures

DP cells resuspended in DMEM with 10%FBS were seeded at a density of $2x10^4$ cell/cm^2 and cultured overnight before establishing the co-culture with hMel, seeded at $2x10^4$ cell/cm^2 in HEM in 0.4µm pore size inserts (Corning). Monocultures of each cell-type were prepared as controls, either by culturing cells in their regular medium, or in the medium used in to establish the co-culture, DMEM with HEM (1:1), to control possible medium effects. Direct co-cultures were established by seeding $3x10^3$ DP cells in round bottom ultra-low attachment 96-wells (Corning) in 50µl of DMEM with 10%FBS for 24 hours before the addition of $1.5x10^3$ hMel resuspended in 25µl of HEM medium. Both co-cultures were performed for 3 days.

DNA, active alkaline phosphatase and ROS quantification

Cells were lysed in water with 0.01% sodium dodecyl sulfate. A 1h incubation at 37ºC was followed by freezing at -80ºC. DNA content was quantified using the Quant-iT™ PicoGreen® dsDNA kit (Thermo Fisher Scientific), and ROS levels were measured using the OxiSelect™ In vitro ROS/RNS assay kit (Cell Biolabs

Inc.). Cell lysates were also used to quantity active ALP in DP cells, using the Alkaline Phosphatase Detection Kit (Sigma-Aldrich). For DNA and ALP quantification in cell aggregates, a 5s sonication step (ice) was first performed to ensure the complete disintegration of the 3D-aggregates prior quantification. All commercial kits were used according to the manufacturer instructions. DNA values were used to normalize ROS and ALP results.

Alkaline phosphatase staining

The detection of active ALP was performed by incubating formalin-fixed DP cells (15min, RT) for 20 minutes with a solution prepared with 5µL of NBT and 3.75µL of BCIP (Roche) in 1 mL of NTMT buffer (100mM NaCl, 100mM Tris-HCl (pH 9.5) and 50mM $MgCl_2$ in water). Representative images were acquired with an AxioVert.A1 microscope (Zeiss).

ELISA

After co-culture, inserts containing the hMel were removed and DP cells were cultured in serum-free DMEM for 24h. The cells supernatant was then collected, centrifuged (3000rpm, 10min) and single-use aliquots were stored at -80ºC. Human VEGF ELISA Development Kit (Peprotech) and Human BMP-2 Standard ELISA Development Kit (Petrotech) were then used following the manufacturer instructions to determine VEGF and BMP2 levels. DNA values were used to normalize data.

Immunofluorescence staining

DP-hMel aggregates were fixed in 10%-formalin (overnight, 4ºC), embedded in HistoGel™ (Thermo Scientific) and processed for paraffin inclusion. 4-µm paraffin-embedded sections were then dewaxed and heat-mediated antigen retrieval was performed with sodium citrate buffer (pH 6.0). Primary antibodies (Table S1) were detected with Alexa Fluor®488/594 (1:500, Molecular Probes) secondary antibodies and nuclear counterstain was performed with DAPI. Images were acquired using an Axio Imager Z1m microscope (Zeiss).

Haematoxylin and eosin (H&E) staining was performed according to standard protocols and representative images acquired with a DM750 microscope (Leica). Images were used to count cell nuclei and determine the DP cells/hMel ratio present within the cell aggregates for normalization of tyrosinase and ALP activity using the DNA amount of the corresponding cells.

Statistical analysis

Statistical analysis and data visualization were performed using the GraphPad Prism 7.03 (San Diego, USA). The D'Agostino & Pearson normality test was used to determine if data followed a Gaussian distribution. Nonparametric data were analysed with a two-tailed Mann-Whitney test (two groups, unpaired) or with a Friedman (paired) or Kruskal-Wallis test (unpaired) when more than 2 groups were compared. Parametric data were analysed with a two-tailed Student's *t*-test (two groups, paired or unpaired). The comparison of more than two groups was performed with an ordinary (unpaired) or RM

(paired) one-way ANOVA (one independent variable) or two-way ANOVA (two independent variables). Data are presented as mean ± standard error of the mean (SEM). For data displayed as dot plots, black dots represent data points and red bars indicate the mean. Differences with *p*-values< 0.05 were considered significant.

Declarations

Acknowledgements

We would like to acknowledge Dr Luca Gasperini for his technical assistance in the image analysis using the CellProfiler™ software.

Authors' contributions

CA – conceptualization, investigation, methodology, data curation, formal analysis, visualization, writing-original draft preparation; **APM –** funding acquisition, project administration, resources, conceptualization, supervision, validation, writing – review & editing; **RLR –** resources, funding acquisition

Funding

This study was support by FCT/MCTES (*Fundação para a Ciência e a Tecnologia/ Ministério da Ciência, Tecnologia, e Ensino Superior*) through the PD/59/2013, PD/BD/113800/2015 (C. Abreu) and IF/00945/2014 (A. P. Marques) grants.

Availability of data and materials

The datasets used and/or analyzed during the current study are available from the corresponding author on reasonable request.

Ethics approval and consent to participate

HF occipital scalp samples were obtained following a protocol approved by the Ethics Committees of the 3Bs Research Group and Sanare Unicapilar Clínica. Informed consent was obtained from each patient.

Consent for publication

All authors read and approved the paper.

Competing interests

The authors declare that they have no competing interests.

References

1. Driskell RR, Clavel C, Rendl M, Watt FM. Hair follicle dermal papilla cells at a glance. J Cell Sci. J Cell Sci; 2011;124(8):1179–82.
2. Slominski A, Wortsman J, Plonka PM, Schallreuter KU, Paus R, Tobin DJ. Hair Follicle Pigmentation. J Invest Dermatol. 2005;124(1):13–21.
3. Tobin DJ, Slominski A, Botchkarev V, Paus R. The Fate of Hair Follicle Melanocytes During the Hair Growth Cycle. J Investig Dermatology Symp Proc. 1999;4(3):323–32.
4. Slominski A, Paus R, Costantino R. Differential Expression and Activity of Melanogenesis-Related Proteins During Induced Hair Growth in Mice. J Invest Dermatol. 1991;96(2):172–9.
5. Ideta R, Soma T, Tsunenaga M, Ifuku O. Cultured human dermal papilla cells secrete a chemotactic factor for melanocytes. J Dermatol Sci. 2002;28(1):48–59.
6. Randall VA, Jenner TJ, Hibberts NA, De Oliveira IO, Vafaee T. Stem cell factor/c-Kit signalling in normal and androgenetic alopecia hair follicles. J Endocrinol. 2008;197(1):11–23.
7. Glover JD, Knolle S, Wells KL, Liu D, Jackson IJ, Mort RL, et al. Maintenance of distinct melanocyte populations in the interfollicular epidermis. Pigment Cell Melanoma Res. 2015;28(4):476–80.
8. Lim J, Ng KJ, Clavel C. Dermal papilla regulation of hair growth and pigmentation. Elsevier; 2019. p. 115–38.
9. Balafa C, Smith-Thomas L, Phillips J, Moustafa M, George E, Blount M, et al. Dopa oxidase activity in the hair, skin and ocular melanocytes is increased in the presence of stressed fibroblasts. Exp Dermatol. 2005;14(5):363–72.
10. Buffey JA, Messenger AG, Taylor M, Ashcroft ATT, Westgate GE, Neil S MAC. Extracellular matrix derived from hair and skin fibroblasts stimulates human skin melanocyte tyrosinase activity. Br J Dermatol. 1994;131(6):836–42.
11. Tobin DJ. The cell biology of human hair follicle pigmentation. Pigment Cell Melanoma Res. 2011;24(1):75–88.
12. Carreau A, Hafny-Rahbi B El, Matejuk A, Grillon C, Kieda C. Why is the partial oxygen pressure of human tissues a crucial parameter? Small molecules and hypoxia. J Cell Mol Med. 2011;15(6):1239–53.
13. Place TL, Domann FE, Case AJ. Limitations of oxygen delivery to cells in culture: An underappreciated problem in basic and translational research. Free Radic. Biol. Med. Elsevier Inc.; 2017. p. 311–22.
14. Dröge W. Free Radicals in the Physiological Control of Cell Function. Physiol Rev. 2002;82(1):47–95.
15. Bartosz G. Reactive oxygen species: Destroyers or messengers? Biochem Pharmacol. 2009;77(8):1303–15.
16. Sena LA, Chandel NS. Physiological Roles of Mitochondrial Reactive Oxygen Species. Mol Cell. 2012;48(2):158–67.
17. Trüeb RM. Oxidative stress in ageing of hair. Int. J. Trichology. Wolters Kluwer – Medknow Publications; 2009. p. 6–14.

18. Upton JH, Hannen RF, Bahta AW, Farjo N, Farjo B, Philpott MP. Oxidative Stress–Associated Senescence in Dermal Papilla Cells of Men with Androgenetic Alopecia. J Invest Dermatol. 2015;135(5):1244–52.
19. Jagannathan L, Cuddapah S, Costa M. Oxidative Stress Under Ambient and Physiological Oxygen Tension in Tissue Culture. Curr Pharmacol Reports. 2016;2(2):64–72.
20. Kanayama K, Takada H, Saito N, Kato H, Kinoshita K, Shirado T, et al. Hair Regeneration Potential of Human Dermal Sheath Cells Cultured Under Physiological Oxygen. Tissue Eng Part A. Mary Ann Liebert Inc; 2020;ten.tea.2019.0329.
21. Xia L, Liu Q, Zhang W, Zhou G, Cao Y, Liu W. Enhanced proliferation and functions of in vitro expanded human hair follicle outer root sheath cells by low oxygen tension culture. Tissue Eng - Part C Methods. Mary Ann Liebert Inc.; 2012;18(8):603–13.
22. Zheng M, Jang Y, Choi N, Kim DY, Han TW, Yeo JH, et al. Hypoxia improves hair inductivity of dermal papilla cells via nuclear NADPH oxidase 4-mediated reactive oxygen species generation'. Br J Dermatol. 2019;181(3):523–34.
23. Horikoshi T, Balin AK, Carter DM. Effects of Oxygen Tension on the Growth and Pigmentation of Normal Human Melanocytes. J Invest Dermatol. 1990;96(6):841–4.
24. Wang W, Winlove CP, Michel CC. Oxygen Partial Pressure in Outer Layers of Skin of Human Finger Nail Folds. J Physiol. 2003;549(3):855–63.
25. Lartigau E, Randrianarivelo H, Avril M-F, Margulis A, Spatz A, Eschw??ge F, et al. Intratumoral oxygen tension in metastatic melanoma. Melanoma Res. 1997;7(5):400–6.
26. Lemasters JJ, Ramshesh VK, Lovelace GL, Lim J, Wright GD, Harland D, et al. Compartmentation of Mitochondrial and Oxidative Metabolism in Growing Hair Follicles: A Ring of Fire. J Invest Dermatol. 2017;137(7):1434–44.
27. Carrasco E, Calvo MI, Blázquez-Castro A, Vecchio D, Zamarrón A, de Almeida IJD, et al. Photoactivation of ROS Production In Situ Transiently Activates Cell Proliferation in Mouse Skin and in the Hair Follicle Stem Cell Niche Promoting Hair Growth and Wound Healing. J Invest Dermatol. 2015;135(11):2611–22.
28. Higgins CA, Richardson GD, Ferdinando D, Westgate GE, Jahoda CAB. Modelling the hair follicle dermal papilla using spheroid cell cultures. Exp Dermatol. 2010;19(6):546–8.
29. Higgins CA, Chen JC, Cerise JE, Jahoda CAB, Christiano AM. Microenvironmental reprogramming by three-dimensional culture enables dermal papilla cells to induce de novo human hair-follicle growth. Proc Natl Acad Sci. 2013;110(49):19679–88.
30. Young T-H, Lee C-Y, Chiu H-C, Hsu C-J, Lin S-J. Self-assembly of dermal papilla cells into inductive spheroidal microtissues on poly(ethylene-co-vinyl alcohol) membranes for hair follicle regeneration. Biomaterials. Biomaterials; 2008;29(26):3521–30.
31. Rushan X, Fei H, Zhirong M, Yu-zhang W. Identification of proteins involved in aggregation of human dermal papilla cells by proteomics. J Dermatol Sci. 2007;48(3):189–97.

32. Messenger AG. Isolation, culture and in vitro behavior of cells isolated from papillae of human hair follicles. Trends Hum Hair Growth Alopecia Res. Springer Netherlands; 1989. p. 57–66.
33. Messenger AG, Jennifer H, Bleehen SS. The in vitro properties of dermal papilla cell lines established from human hair follicles. Br J Dermatol. 1986;114(4):425–30.
34. Ohyama M, Kobayashi T, Sasaki T, Shimizu A, Amagai M. Restoration of the intrinsic properties of human dermal papilla in vitro. J Cell Sci. 2012;125(17):4114–25.
35. Slominski A, Paus R. Melanogenesis is coupled to murine anagen: Toward new concepts for the role of melanocytes and the regulation of melanogenesis in hair growth. J Invest Dermatol. 1993;101(1):S90–7.
36. Iida M, Ihara S, Matsuzaki T. Hair cycle-dependent changes of alkaline phosphatase activity in the mesenchyme and epithelium in mouse vibrissal follicles. Dev Growth Differ. 2007;49(3):185–95.
37. Lachgar, Charveron, Gall, Bonafe. Minoxidil upregulates the expression of vascular endothelial growth factor in human hair dermal papilla cells. Br J Dermatol. 1998;138(3):407–11.
38. Yano K, Brown LF, Detmar M. Control of hair growth and follicle size by VEGF-mediated angiogenesis. J Clin Invest. 2001;107(4):409–17.
39. Botchkarev VA, Botchkareva N V., Roth W, Nakamura M, Chen L-H, Herzog W, et al. Noggin is a mesenchymally derived stimulator of hair-follicle induction. Nat Cell Biol. 1999;1(3):158–64.
40. Soma T, Tajima M, Kishimoto J. Hair cycle-specific expression of versican in human hair follicles. J Dermatol Sci. 2005;39(3):147–54.
41. Wagner BA, Venkataraman S, Buettner GR. The rate of oxygen utilization by cells. Free Radic Biol Med. 2011;51(3):700–12.
42. Chen Q, Fischer A, Reagan JD, Yan LJ, Ames BN. Oxidative DNA damage and senescence of human diploid fibroblast cells. Proc Natl Acad Sci. 1995;92(10):4337–41.
43. Huang W-Y, Huang Y-C, Huang K-S, Chan C-C, Chiu H-Y, Tsai R-Y, et al. Stress-induced premature senescence of dermal papilla cells compromises hair follicle epithelial-mesenchymal interaction. J Dermatol Sci. 2017;86(2):114–22.
44. Mecklenburg L, Tobin DJ, Müller-Röver S, Handjiski B, Wendt G, Peters EMJ, et al. Active Hair Growth (Anagen) is Associated with Angiogenesis. J Invest Dermatol. Blackwell Publishing Inc.; 2000;114(5):909–16.
45. Botchkarev VA, Botchkareva N V., Nakamura M, Huber O, Funa K, Lauster R, et al. Noggin is required for induction of the hair follicle growth phase in postnatal skin. FASEB J. 2001;15(12):2205–14.
46. Tobin DJ, Gunin A, Magerl M, Handijski B, Paus R. Plasticity and cytokinetic dynamics of the hair follicle mesenchyme: Implications for hair growth control. J Invest Dermatol. Blackwell Publishing Inc.; 2003;120(6):895–904.
47. Jahoda CAB, Oliver RF. Vibrissa dermal papilla cell aggregative behaviour in vivo and in vitro. J Embryol Exp Morphol. 1984;79:211–24.

48. Commo S, Bernard BA. Melanocyte Subpopulation Turnover During the Human Hair Cycle: An Immunohistochemical Study. Pigment Cell Res. 2000;13(4):253–9.
49. Kim JW, Ho WJ, Wu BM. The role of the 3D environment in hypoxia-induced drug and apoptosis resistance. Anticancer Res. 2011;31(10):3237–45.
50. Leek R, Grimes DR, Harris AL, McIntyre A. Methods: Using Three-Dimensional Culture (Spheroids) as an In Vitro Model of Tumour Hypoxia. Adv Exp Med Biol. 2016. p. 167–96.
51. Diehl C. Melanocytes and Oxidative Stress. J Pigment Disord. 2014;1(4):1512–1518.
52. Denat L, Kadekaro AL, Marrot L, Leachman SA, Abdel-Malek ZA. Melanocytes as Instigators and Victims of Oxidative Stress. J Invest Dermatol. 2014;134(6):1512–8.
53. Gledhill K, Gardner A, Jahoda CAB. Isolation and Establishment of Hair Follicle Dermal Papilla Cell Cultures. Methods Mol Biol. Methods Mol Biol; 2013. p. 285–92.
54. Lamprecht MR, Sabatini DM, Carpenter AE. CellProfiler™: free, versatile software for automated biological image analysis. Biotechniques. 2007;42(1):71–5.

Figures

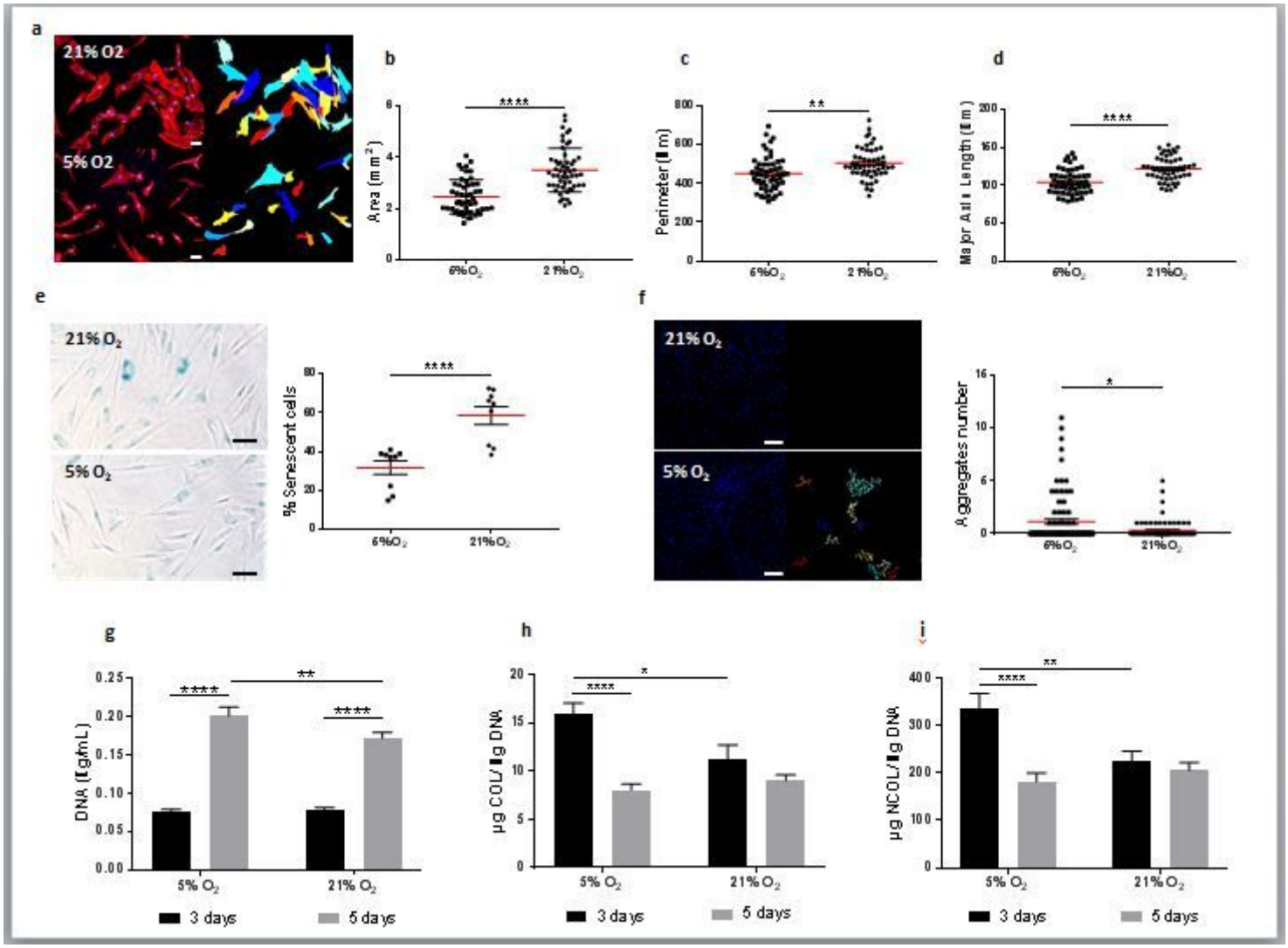

Figure 1

DP cells phenotype under physoxia. (a) Representative images of DP cells F-actin cytoskeleton labelled with Phaloidin-TRITC (left panel) and respective CellProfilerTM output (right panel) used to quantify morphological features such as (b) cell area, (c) perimeter and (d) major axis length. Nuclei were counterstained with DAPI. Significant differences between DP cells cultured under normoxia (21%O2) or physoxia (5%O2) were analysed using an unpaired, two-tailed Student's t-test (n= 3). Scale bar= 50 µm. (e) Representative images of the β-galactosidase staining used to quantify the percentage of senescent DP cells. Significant differences were analysed using a paired, two-tailed Student's t-test (n= 3). Scale bar= 50µm. (f) Representative images of DAPI labelled DP cells (left panel) and CellProfilerTM output of subsequent grouping of related nuclei (distance< 8 pixels) used to count the number of cell aggregates (≥30 related nuclei). Significant differences were analysed using an unpaired, two-tailed Mann-Whitney test (n= 3). Scale bar= 200µm. (g) DNA quantification used to evaluate cellular proliferation. Differences among oxygen levels at the same time point and differences for the same oxygen level along time were analysed using an unpaired, two-tailed Mann-Whitney test (n= 3). Quantification of (h) collagenous (COL) and (i) non-collagenous (NCOL) proteins secretion. Results were analysed using an unpaired, two-way ANOVA. All data is presented as mean ± SEM and statistical differences are indicated as *p<0.05; **p<0.01; ****p<0.0001

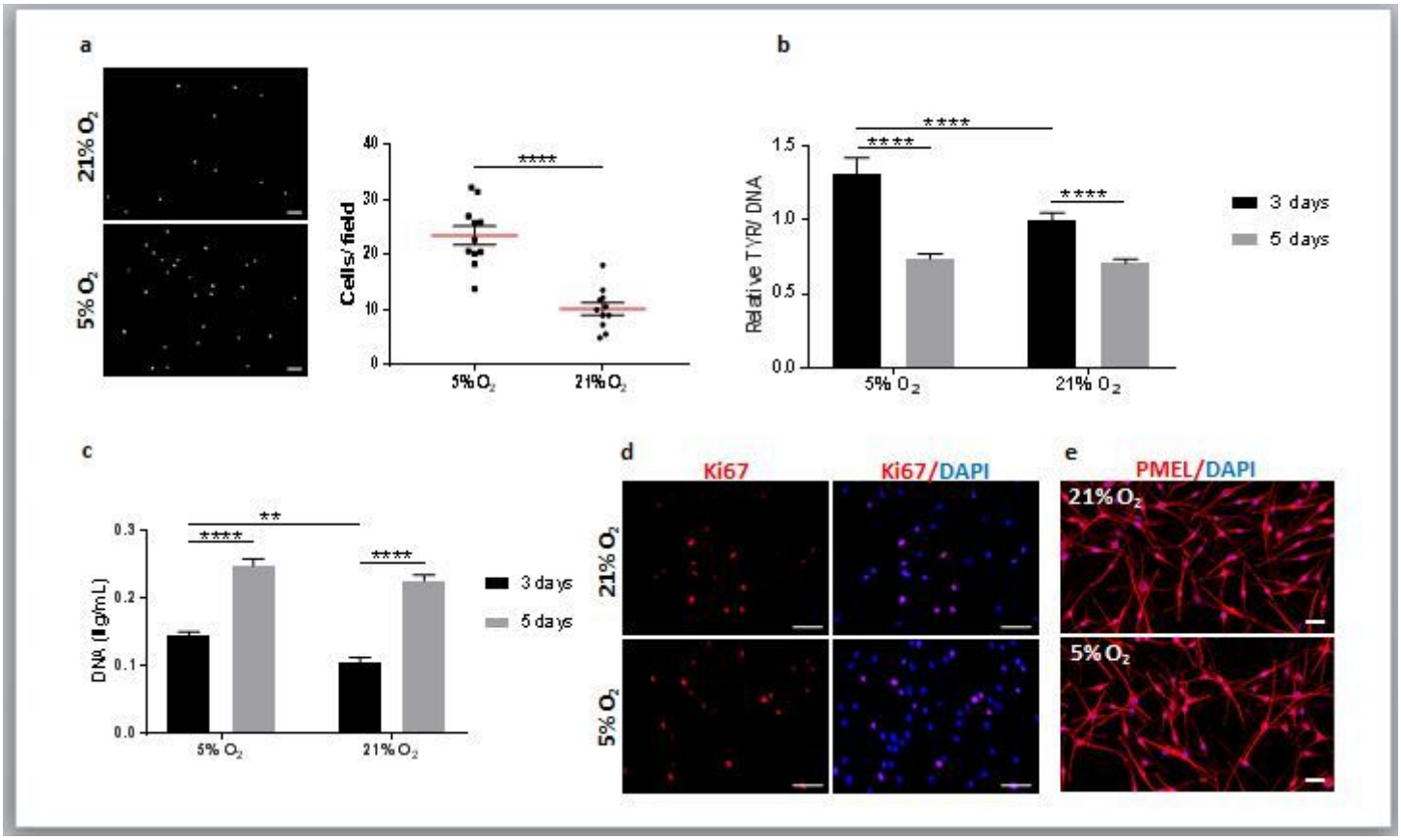

Figure 2

Characterization of hMel behaviour under physoxia. (a) Representative fluorescence microscopy images of DAPI labelled hMel that migrated over 48h and respective quantification. Scale bar= 100 µm. (b) Quantification of hMel tyrosinase activity (TYR). Relative values in comparison to cells cultured under 21%O2 at day 3 of culture are presented. Significant differences were determined by a paired, two-way ANOVA (n= 3). (c) DNA quantification used to assess hMel cellular proliferation. Significant differences were analysed using an unpaired, two-way ANOVA (n= 3). (d) Representative immunofluorescence images showing ki67-positive hMel. Nuclei were counterstained with DAPI. Scale bar= 50µm. (e) PMEL immunostaining showing hMel morphology. Nuclei were counterstained with DAPI. Scale bar= 50µm. Significant differences were analysed using a paired, two-tailed Student's t-test (n= 3). All data is presented as mean ± SEM and statistical differences are indicated as **p<0.01; ****p<0.0001

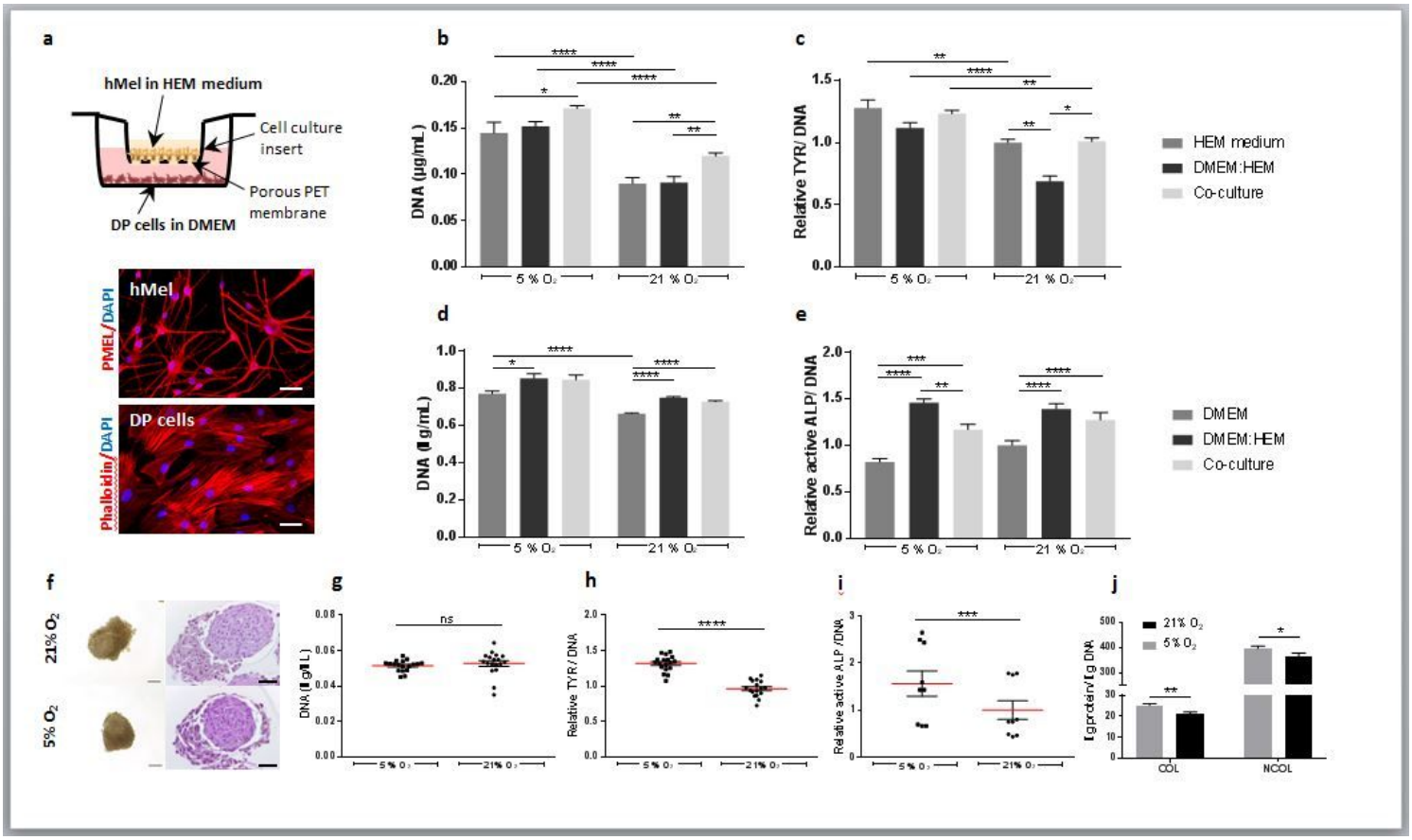

Figure 3

Physoxia effects on co-cultured hMel and DP cells. (a) Schematic representation of the indirect co-culture system used to study hMel and DP cells interactions, accompanied by images displaying the morphology of each cell type, respectively immunolabelled with PMEL and stained with Phalloidin-TRITC. Nuclei were counterstained with DAPI. Scale bar= 50µm. (b) DNA quantification used to assess hMel cell numbers in the co-culture with DP cells, and in the respective homotypic controls – hMel cultured in standard conditions (HEM medium) or in the medium used for the co-culture (DMEM:HEM). Data were analysed using an unpaired, one-way ANOVA (n= 3). (c) Quantification of tyrosinase activity (TYR) in hMel in the different culture conditions. Statistical differences were calculated using an unpaired, Kruskal-Wallis test (n= 3). Quantification of (d) DNA and (e) active ALP of DP cells co-cultured with hMel and in the

respective control media. Significant differences were analysed using a paired, Friedman test (n= 6 for DNA; n= 3 for active ALP). (f) Representative phase contrast (left panel) and H&E (right panel) images of the cell aggregates formed after direct culture of hMel with DP spheroids. Scale bars are 100µm and 50µm, respectively. (g) Quantification of DNA of the aggregates. P values were calculated using an unpaired, two-tailed Mann-Whitney test (n= 3). (h) Quantification of hMel tyrosinase activity (TYR) in the aggregates. Differences were calculated using a paired, two-tailed Student's t-test (n= 3). (i) Quantification of active ALP in the DP spheroids. A paired two-tailed Student's t-test was used to perform the statistical analysis (n= 3). (j) Quantification of COL and NCOL proteins present in the aggregates. Statistical analysis was performed using a paired Wilcoxon signed-rank test (COL) or a paired two-tailed Student's t-test (NCOL) (n= 4). Relative values are presented in comparison to the cells standard culture conditions at 21%O2 (c,d) or in comparison to aggregates formed at 21%O2 (h,i). All data is presented as mean ± SEM and statistical differences are indicated as *p<0.05; **p<0.01; ***p<0.001; ****p<0.0001

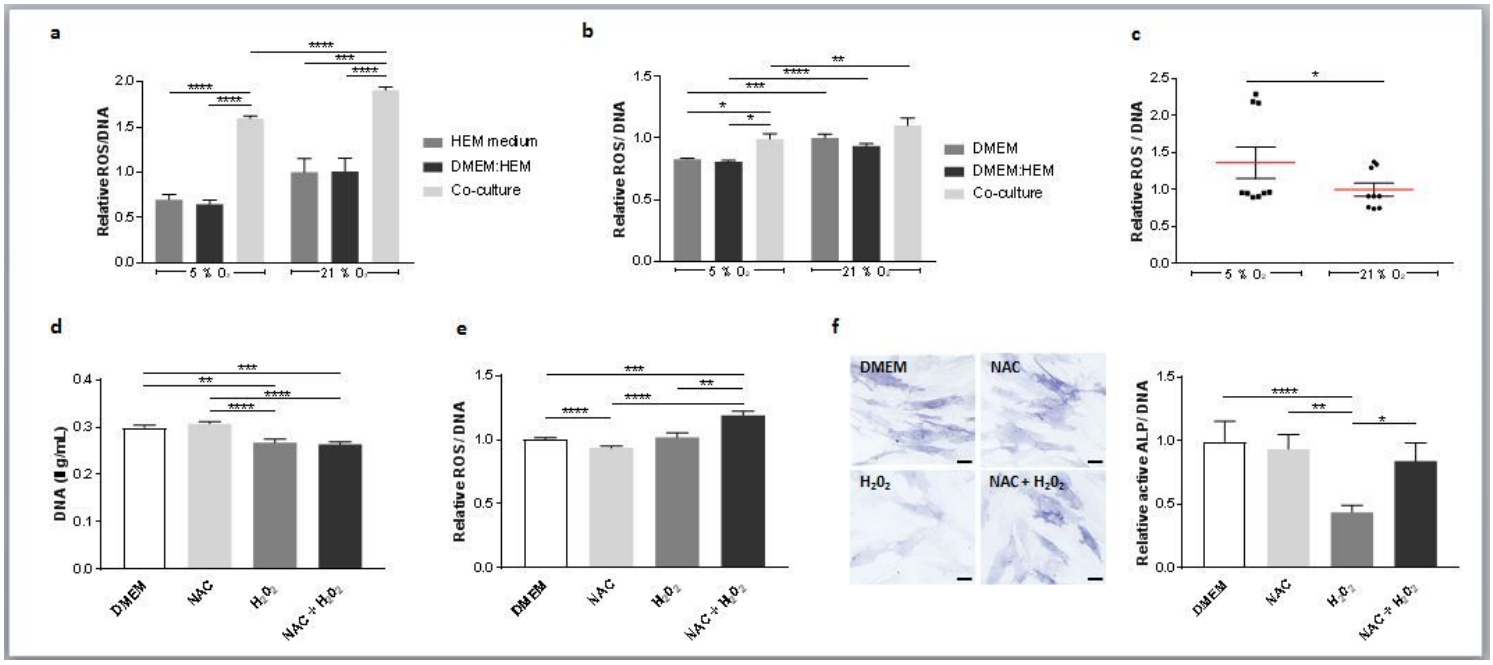

Figure 4

ROS production by co-cultured hMel and DP cells and analysis of its association to active ALP in DP cells. ROS quantification in (a) hMel and (b) DP cells co-cultured indirectly and in the respective control conditions. Significant differences were analysed using an unpaired, one-way ANOVA (n= 3). (c) Amount of ROS in the DP-hMel cell aggregates. Statistical analysis was performed using a paired, two-tailed Student's t-test (n= 3). (d) Quantification of the DNA amount in conventionally cultured DP cells (DMEM, 21%O2) in the presence of the ROS-scavenger N-acetyl cysteine (NAC), hydrogen peroxide (H2O2) or the combination of both (NAC+H2O2). A paired Friedman test was used to identify significant differences (n= 3). (e) Quantification of ROS production by DP cells after NAC, H2O2 or both treatments. Statistical analysis was performed using a paired, one-way ANOVA (n= 3). (f) Representative light microscopy images of ALP staining in DP cells and respective quantification of active ALP levels. Significant differences were calculated using a paired, Friedman test (n= 3). Scale bar= 100µm. Relative values are

presented in comparison to the cells standard culture conditions at 21%O2 (a,b,e,f) or in comparison to aggregates formed at 21%O2 (c). All data is presented as mean ± SEM and statistical differences are indicated as *p<0.05; **p<0.01; ***p<0.001; ****p<0.0001

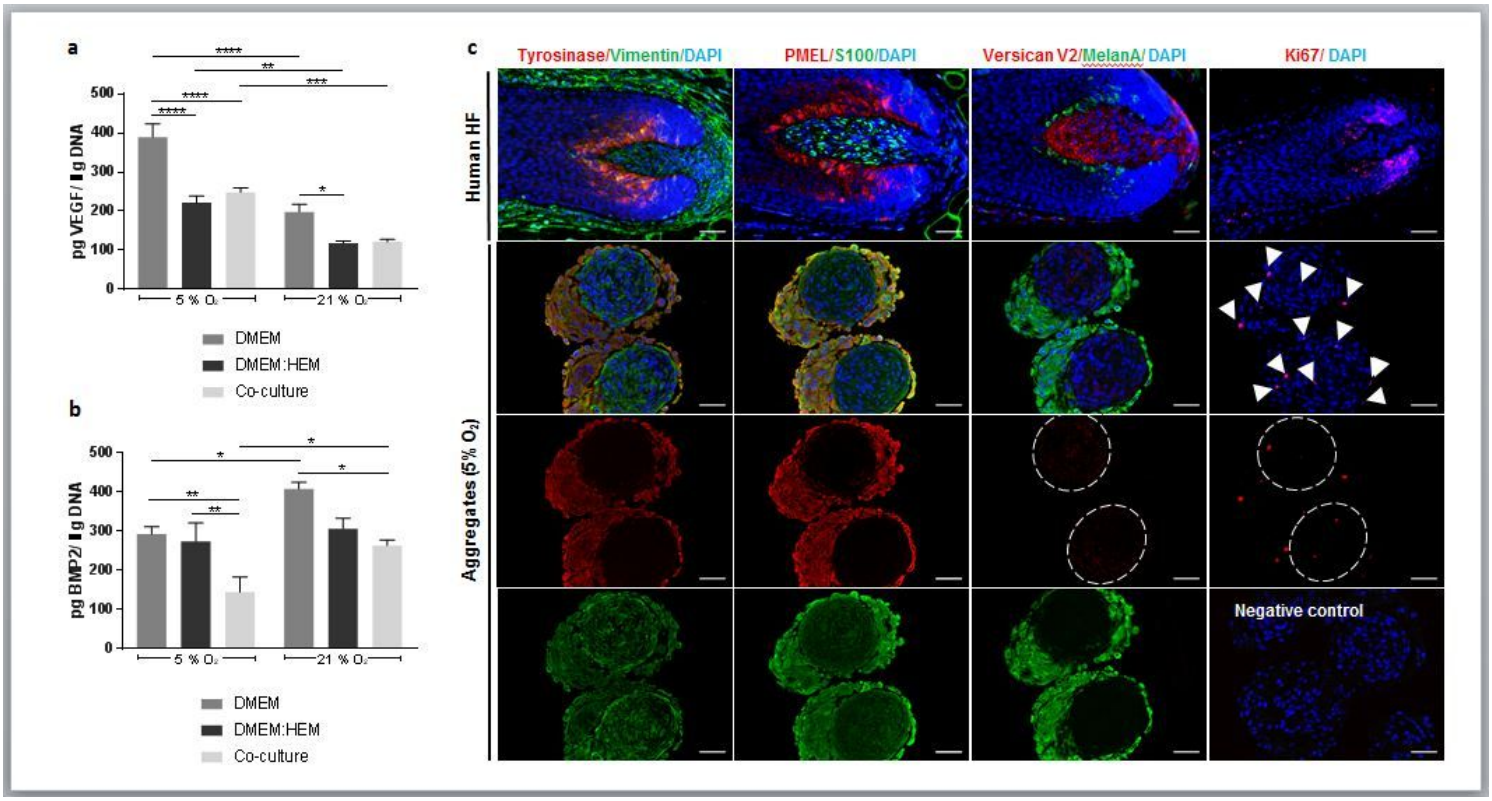

Figure 5

Phenotypic assessment of co-cultured DP cells and hMel. ELISA quantification of (a) VEGF and (b) BMP2 released by DP cells indirectly co-cultured with hMel and the respective control conditions. Results are shown as mean ± SEM. Significant differences were analysed using an unpaired, one-way ANOVA (n= 3) and are indicated as *p<0.05; **p<0.01; ***p<0.001; ****p<0.0001. (c) Representative immunofluorescence images showing the expression of different DP cells and hMel markers in the native hair follicle (HF) tissue and in the DP-HMel aggregates prepared under physoxia. Nuclei were counterstained with DAPI. White arrowheads indicate ki67-positive cells and dotted circles delimitate the DP spheroid area. Scale bars= 50µm

Supplementary Files

This is a list of supplementary files associated with this preprint. Click to download.

- Supplementaryinformation.docx